Neutron Resonance Spectroscopy. IX. The Separated Isotopes of Samarium and Europium*

F. Rahn, H. S. Camarda,† G. Hacken, W. W. Havens, Jr., H. I. Liou, J. Rainwater, M. Slagowitz, and S. Wynchank‡
Columbia University, New York, New York 10027

(Received 2 February 1972)

Neutron transmission and self-indication measurements have been made for two of the separated isotopes of Sm ($A=152$ and 154) and the separated isotopes of Eu ($A=151$ and 153) at the Nevis synchrocyclotron. The measurements used a 200-m path for transmission measurements and a 40-m path for self-indication measurements, covering an energy range from approximately 1 eV to greater than 5 keV. Since these isotopes are at a region of a peak in the $l=0$ strength function, mainly s resonances are involved. The results for the even-even Sm isotopes show that essentially complete s populations were obtained for the first 70 levels in Sm^{152} and 27 levels in Sm^{154}. Values of Γ_n (or $g\Gamma_n$ for Eu) were obtained for the observed resonances. Values of Γ_γ, obtained for 9, 3, 45, and 46 levels of Sm^{152}, Sm^{154}, Eu^{151}, and Eu^{153}, respectively, give $\langle\Gamma_\gamma\rangle$ values of 65, 79, 90.0, and 94.8 meV, respectively, with most of the individual values within 20% of $\langle\Gamma_\gamma\rangle$. The s strength function is $10^4 S_0 = 2.2\pm0.4$, 1.8 ± 0.5, 3.2 ± 0.5, and 2.3 ± 0.4 for $Sm^{152}(n=90)$, $Sm^{154}(n=33)$, $Eu^{151}(n=63)$, and $Eu^{153}(n=68)$, where n is the number of levels in the sample. Somewhat smaller S_0 values result for the Sm isotopes if a larger energy interval is used. Values of the mean s level spacing for these isotopes of 51.8 ± 1.5, 115 ± 8, ~0.7, and ~1.1 eV, respectively, were found. Good fits are obtained with the Porter-Thomas theory for the reduced-neutron-width distributions and the Wigner formula for the nearest-neighbor level separation. Other statistical tests applied to Sm^{152} and Sm^{154}, respectively, are: (a) the Dyson-Mehta Δ statistic, which is particularly sensitive to long-range order in the level spacings, $\Delta=0.40$ and 0.38 versus $\Delta_{DM}=0.42\pm0.11$ and 0.32 ± 0.11; (b) correlation coefficients of adjacent nearest-neighbor spacings are -0.26 ± 0.10 and -0.32 ± 0.18 versus -0.27 predicted for an orthogonal ensemble.

I. INTRODUCTION

This is the ninth in a series[1] of papers presenting the results of high-intensity and high-resolution neutron-spectroscopy measurements using the neutron velocity spectrometer at the Columbia University synchrocyclotron. Preliminary results for Sm and Eu were given in the thesis of Rahn.[2] The thesis results have been carefully reviewed and the analysis has been expanded. The details of the experimental system and data-analysis procedures have been published in the preceding Paper VIII of this series, and therefore will only be reviewed briefly. The reader is directed to our earlier papers for more specific information.

The Sm and Eu results presented here are of particular interest in that they help to complete our knowledge of the systematics of neutron resonance reactions in the rare-earth region of the Periodic Table, and provide good tests for various statistical theories of the nucleus. The mass numbers $151 \leq A \leq 154$ occur close to a relative maximum of the s strength function S_0 and a relative minimum of the p strength function S_1. They therefore represent good experimental situations where few if any p resonances are observed, and are suitable for testing the various statistical predictions concerning fluctuations of the reduced neutron widths and adjacent level spacings. For the even Sm isotopes I is zero and therefore the observed resonances form a single population all having the same Z, A, J, and parity. The single population set of resonances provides a particularly good test for the Dyson-Mehta Δ statistic, which is sensitive to both long- and short-range order of the level spacing distribution. Our recent results (Paper VIII), particularly for Er^{166}, gave the first, and so far the best confirmation of the Dyson-Mehta theory for a statistical "orthogonal ensemble." The Sm^{152} and Sm^{154} results give additional confirmation. The failure to fit the Δ-statistic test before our 1968 experimental results had been obtained was mainly due to a lack of suitably "clean" data covering a large enough complete s-level population near a peak of S_0. Our recent measurements of separated rare-earth isotopes came at a time when substantial improvements in our spectroscopy system were such as to assure high quality of the resulting data. The nature of these theories and the comparisons for the erbium isotopes was discussed in previous papers.[1]

Samarium, $Z = 62$, has seven stable isotopes, with $A = 152$ and 154 contributing 26.45 and 22.33 at.% each to the natural abundance, and both having target spin-parity 0^+. Europium, $Z = 63$, has only the two naturally occurring isotopes $A = 151$ and 153 in nearly equal abundance. Both Eu^{151} and Eu^{153} have spin-parity values of $\frac{5}{2}^+$. By using separated-isotope samples of relatively high purity, we obtain isotope identification and Γ_n resonance parameters for 90 levels in Sm^{152} to 5 keV (vs only one level at 8 eV for which Γ_n has been previously reported), 33 levels in Sm^{154} to 5 keV (vs no previously reported Sm^{154} levels for which Γ_n values were reported), 105 levels in Eu^{151} to 100 eV (vs 27 levels to 27 eV previously reported), and 77 levels in Eu^{153} to 100 eV (vs 19 levels to 24 eV previously reported). Values of Γ_γ were also obtained for many levels, giving relatively good evaluations of the $\langle\Gamma_\gamma\rangle$ for these isotopes. Previous results by a number of investigators have been compiled in the 2nd supplement to Report No. BNL-325.[3] Recently, Karzhavina, Fong, and Popov[4] at Dubna published the resonance energies E_0 for levels up to 2 keV for Sm^{152} and Sm^{154}, but without giving the other level parameters.

The mass numbers $151 \leq A \leq 154$ are close to a peak of the heavy-mass fragments in the fission-product curve. Isotopes with these masses are introduced into nuclear reactors by means of the fission process and subsequent decay chains. Moreover, these isotopes can be used in nuclear reactors to maximize fuel utilization by smoothing neutron-flux profiles and eliminating power peaking. A knowledge of the capture cross section and strength functions of these isotopes is necessary for the design of the next generation of reactors. In addition, experimental values of the s strength function for isotopes in the rare-earth region are useful in the development of the optical model of the nucleus.[5] The quadrupole distortion of these isotopes lead to the splitting of the so-called $4s$ giant resonance, where S_0 has a pronounced dependence on the atomic weight for $A \simeq 150$.

II. EXPERIMENTAL DETAILS

The Columbia University Nevis synchrocyclotron accelerated 70 bunches/sec of protons to ~350 MeV, with a ~1.5-μA time average proton current, during the 1968 operation. When each proton bunch reached ~68-in. orbit radius, it was deflected to give ~1-A proton bursts into a Pb target of ~20-nsec duration. This gave $>10^{19}$ evaporation neutrons/sec during the burst. A water moderator, directly below the Pb target was the effective pulsed-neutron source for a collimated flight path leading to a "flat detector" at 200 m (for transmission measurements), or to a 40-m detector which could be used either for transmission measurements, or for self-indication measurements. A type 6050 ASI (EMR) on-line computer system, having a 16 384-word memory was used in conjunction with an elaborate interface system which provided "clock" and "fast buffering" features. The system permitted simultaneous use of 8192 histogram time-of-flight locations, with variable channel widths in blocks of 512 channels and variable delay. A more complete account of the system and data analysis procedures can be found in Paper VIII of this series.

The measurements described in this paper used separated-isotope samples of Sm^{152}, Sm^{154}, Eu^{151}, and Eu^{153} in $1\frac{1}{4}\times 2\frac{1}{2}$-in. and $2\frac{1}{2}\times 2\frac{1}{2}$-in. slab formats. These particular sizes were a compromise intended to be used also for muonic x-ray studies by a different group. The samples obtained from Oak Ridge National Laboratory were of the chemical form Sm_2O_3 or Eu_2O_3 powder, bonded using a tiny amount of diluted polystyrene ("Q-dope") binder, and packaged in thin Al foil for protection. No natural samples were used. The separated-isotope samples were >95% enriched in the main isotope of the sample. Each isotope sample, as obtained, was made into several smaller samples, so a range of effective sample thicknesses could be used to help in the level parameter analysis. Tables I and II list the various final sample "thicknesses" and composition as used in the transmission position, or in the 40-m "detector sample position." The $1/n$ values in b/atom are the inverse of the isotope thicknesses. For the Sm samples, the levels due to other than the $A = 152$ or 154 Sm isotopes gave contributions of near background size for a few of the stronger levels. The weak $A = 152$ levels in the $A = 154$ sample, and vice versa, were evident and provided additional "very thin" sample information in the resonance-param-

TABLE I. Composition of the separated samarium isotopes (values are for each sample of Sm_2O_3).

Main isotope	Number of samples	g of Sm	$1/n$ values of the isotopes (b/atom): Sm^{144}	Sm^{147}	Sm^{148}	Sm^{149}	Sm^{150}	Sm^{152}	Sm^{154}
Sm^{152}	1	19.8	880 000	165 000	189 000	104 000	99 600	579	7680
Sm^{152}	1	18.6	···	676 000	774 000	454 000	541 000	546	120 000
Sm^{154}	2	10.0	···	241 000	314 000	241 000	431 000	49 500	1072

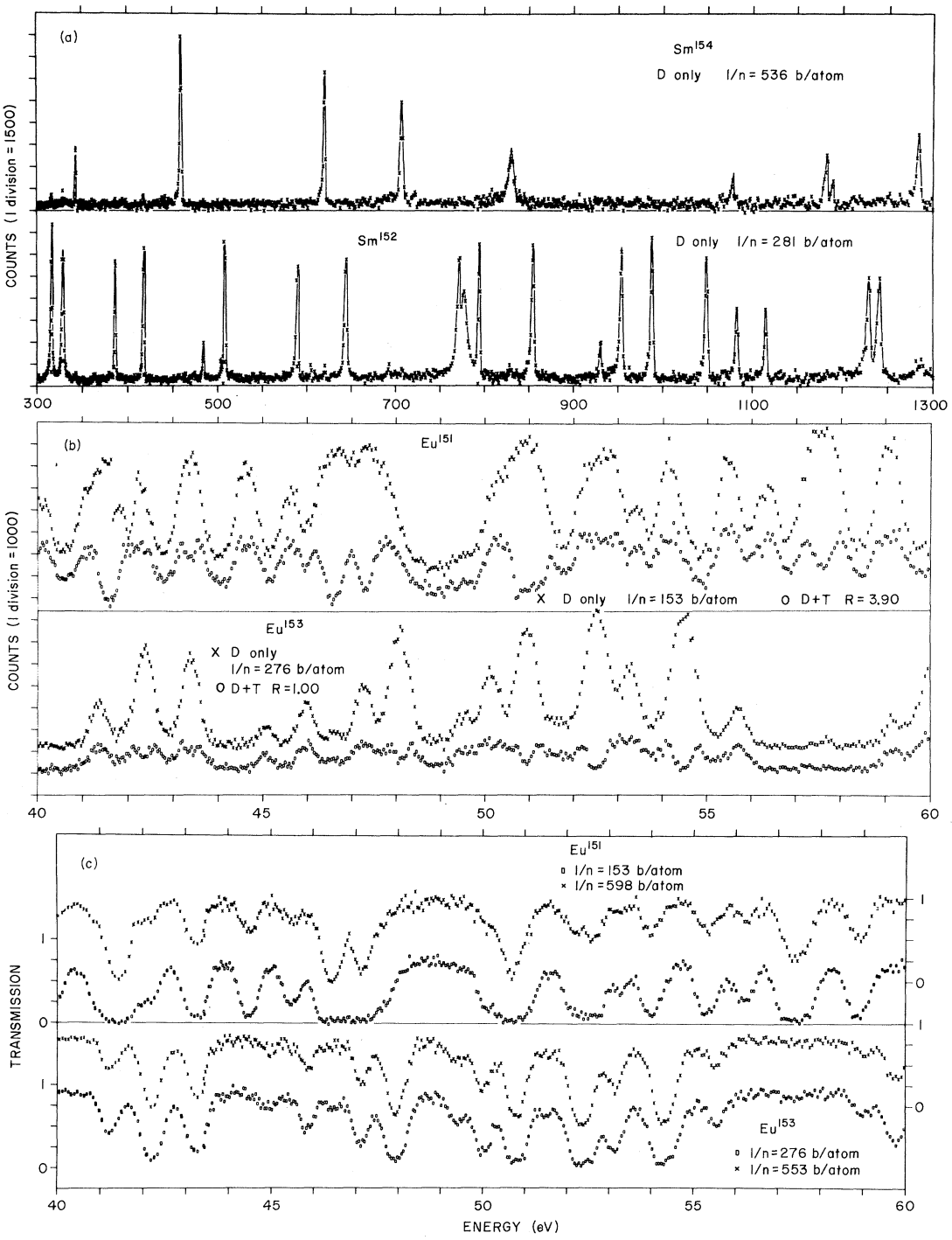

FIG. 1. (a) Examples of the 40-m D-only data, counts versus energy, in the energy region 300 to 1300 eV for Sm^{152} and Sm^{154}. First-order background has been subtracted in these plots. (b) Examples of the 40-m self-indication data, counts versus energy, for Eu^{151} and Eu^{153} in the energy region 40 to 60 eV. The histograms denoted D only are the result of a sample placed in the detector position, and the $D + T$ histogram shows the effect of an additional T sample in the beam, which causes dips to appear at the peaks of the D-only sample. The scales are slightly offset for clarity. The ratio of the D-only thickness to T thickness is denoted by R in the figure. (c) Examples of the 40-m transmission data for Eu^{151} and Eu^{153} in the energy region 40 to 60 eV. The samples were "thin" ($n\sigma \ll 1$) between resonances, but tended to be thick at resonance. Offset scales were used for the various sample thicknesses.

TABLE II. Composition of the separated europium isotopes (values are for each sample of Eu_2O_3).

Main isotope	Number of samples	g of Eu	$1/n$ values of the isotopes (b/atom): Eu^{151}	Eu^{153}
Eu^{151}	2	34.4	153	4680
Eu^{151}	4	7.8	598	183 000
Eu^{153}	2	19.7	21 950	276
Eu^{153}	2	19.8	22 030	277
Eu^{153}	2	10.5	163 000	2048

eter analysis of the data. The Eu samples were so pure that even relatively strong levels in the less abundant isotope of a sample did not "show through" their resonance contribution. The Sm and Eu measurements used only one timing condition for the 200-m detector, covering the energy interval from 5158 to 30 eV. Flat detector measurements at 39.57 m covered the energy interval from 55.6 keV to 0.98 eV, but only the region below ~100 eV was used to extend the lower end of the energy interval from that of the 200-m detector. The 40-m self-indication measurements extended down to 3.05 eV for Sm and 0.81 eV for Eu.

III. EXAMPLES OF THE DATA ANALYSIS

Figure 1 shows examples of our experimental data. Part (a) of this figure shows the background subtracted "D-only" data for Sm^{152} and Sm^{154} from 300 to 1300 eV, while part (b) gives similar plots for the Eu isotopes showing both "D-only" and "$D+T$" information. The upper and lower halves of these plots show the experimental counts per channel obtained for the different isotopes, and illustrate the method of assigning a resonance to its proper isotope. The Sm data showed very weak levels which were identified as due to other Sm isotopes, or impurities, and are not treated in this paper. The assignment for the Eu isotopes is thought to be relatively certain since both stable isotopes were measured. Figure 1(b) shows the counts from thick "D-only" samples at the detector, and the "$D+T$" histogram displays the results of adding a T sample, which causes dips to occur at the peaks of the "D-only" sample. These plots clearly show, for instance, that the peak near 47 eV in Eu^{151} is a doublet, with resonances at $E_0 = 46.41$ and 47.24 eV.

In Eu, the resonances are sufficiently closely spaced so that there is considerable capture occurring between resonance levels. This is observed in our "$D+T$" measurements in which the counting rate at exact resonance for strong levels, where nearly all the neutrons are removed from the beam by the T sample, is lower than the minimum counting rate in the wings of the resonance. There was some concern as to whether this difference was able to be explained in terms of contributions from resonance wings. To test for self-consistency, the expected σ versus E was calculated using the level parameters which we had obtained from the analysis. These calculated results were in good agreement with the observed "D-only" and "$D+T$" background-subtracted data. No extra "nonresonance" capture terms were needed to explain the observed data. This also showed that the background subtraction were performed correctly.

Examples of our transmission data are shown in Fig. 1(c). The samples were "thin" ($n\sigma \ll 1$) between resonances but very thick ($n\sigma > 1$) at resonances, so no attempt was made to generate "true" σ versus E curves through the resonances. Instead, we assume that the Breit-Wigner theory applies and determine the level parameters which are most consistent with the observed effects in the data at resonance.

The strength function, S_0, for these samples is $\langle \Gamma_n^0 \rangle / \langle D \rangle \leq 4 \times 10^{-4}$. For the Eu isotopes $\langle D \rangle \cong 1$ eV and $\Gamma_n \ll \Gamma_\gamma$ below 100 eV. We find $\langle \Gamma_\gamma \rangle \cong 100$ meV, which is comparable to the Doppler width Δ at about 25 eV. Aside from small measurement uncertainties in the individual Γ_γ, the true Γ_γ involve a many-channel phenomenon of the various possible first-step γ-cascade transitions, so the individual Γ_γ should not have large statistical fluctuations about the $\langle \Gamma_\gamma \rangle$ of the population. The Doppler width Δ increases as $E^{1/2}$ and is of the order of 200 meV at $E_0 = 100$ eV for our samples. It poses no special problems for the Sm isotopes studied. For Eu, $\Gamma + \Delta$ is about 300 meV at 100 eV. This value is comparable to the mean observed spacing between levels, so that it is difficult to resolve all levels, particularly above 100 eV. The Wigner level-repulsion effect operates for the levels of the even-even Sm isotopes, but not for the spacing between levels of different spin J for the Eu isotopes.

The analysis requires a choice for the potential scattering length R', which is related to the potential scattering cross section. We used the value $R' = 8.0$ fm obtained from optical-model calculations for the deformed Sm and Eu isotopes. This single value was used for all cases, since the range of A values is quite small. The Sm resonance analysis is only weakly affected, while the Eu level analysis is insensitive to our choice of R'. The value of R' used is in agreement with recent experimental results of Pineo[6] at Duke University.

The transmission and self-indication values obtained for a series of sample thicknesses usually determine a unique set of resonance parameters

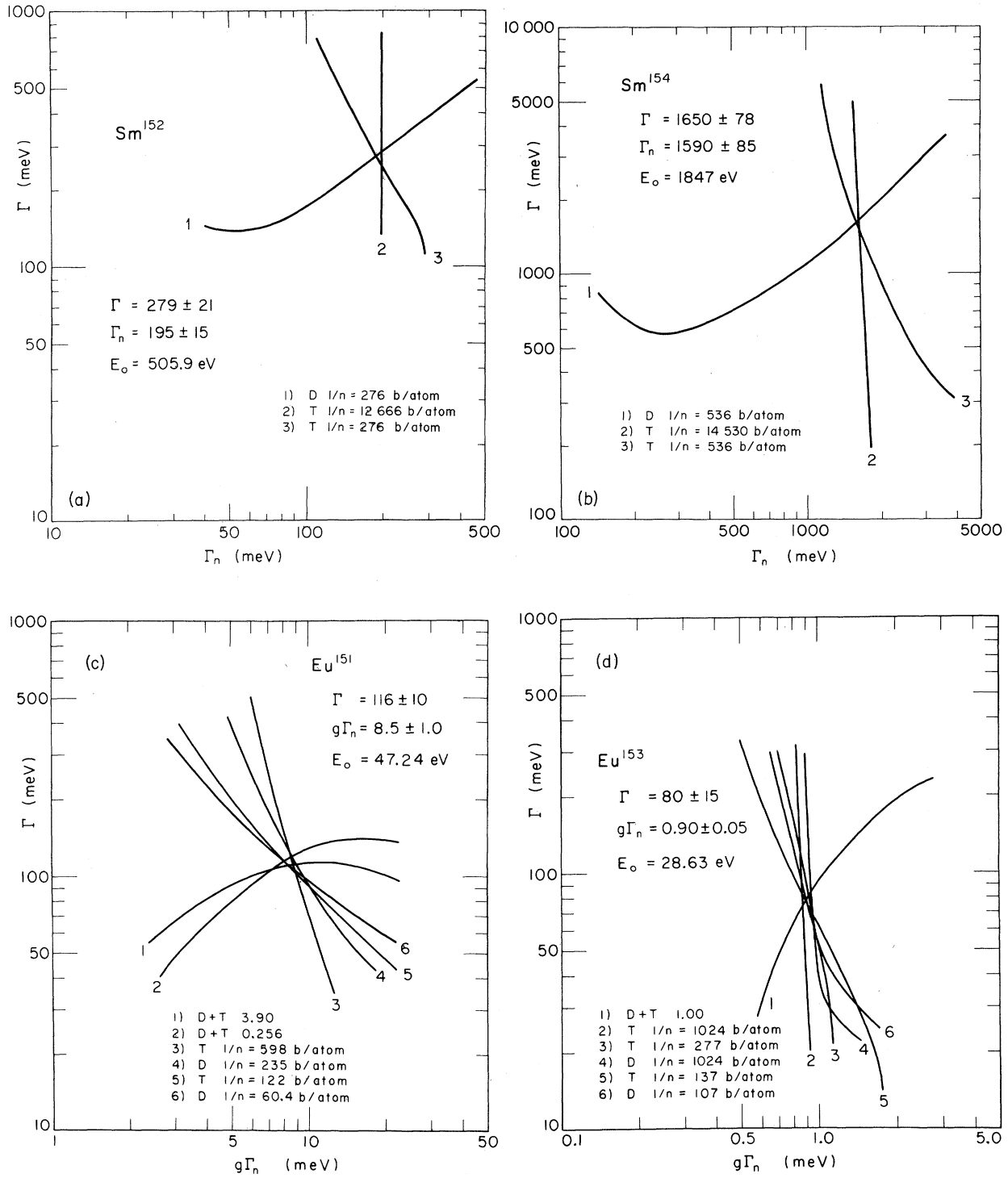

FIG. 2. (a)–(d) Examples of the level-parameter analysis for levels in Sm^{152}, Sm^{154}, Eu^{151}, and Eu^{153}, respectively. For each level there are several curves, showing the implied relationship between $g\Gamma_n$ and Γ derived from the transmission and self-indication data. Curves from the transmission data are labeled T, followed by the inverse thickness $(1/n)$ value of the sample; curves from the D-only data are labeled D, followed by the $(1/n)$ value of the sample; and curves derived from the self-indication data are labeled $(D+T)$, followed by the thickness ratio, R, of the D sample to the T sample. The intersection of the curves implies the values of both Γ and $g\Gamma_n$ in favorable cases.

consistent with the experimental information. In favorable cases, both the capture width Γ_γ and the product $g\Gamma_n$ are determined. For Sm^{152} and Sm^{154}, $I=0$, $J=(\frac{1}{2})^+$, and $g=1$ for all levels. For levels where Γ_γ could not be determined, a value of $g\Gamma_n$ is obtained by setting $\Gamma_\gamma=\langle\Gamma_\gamma\rangle$ for the isotope, using the fact that capture is a many-channel process, so that individual Γ_γ values have relatively small fractional fluctuations about $\langle\Gamma_\gamma\rangle$, while Γ_n can fluctuate by large fractional amounts about $\langle\Gamma_n\rangle$. The resonances of Eu^{151} and Eu^{153} isotopes have two possible spin assignments, $J=2$ or 3. However, the high target spin along with the relatively weak Γ_n implied by the close level spacings make spin assignments highly uncertain, and it is satisfactory to use the mean, $\langle g\rangle=\frac{1}{2}$, for all levels.

Recent capture-γ studies on a range of nuclei have suggested that the compound-nucleus spin state can be determined with high reliability from a study of the ratios of the strengths of selected transitions in the γ-cascade process. Such studies for the Eu isotopes would be helpful if the γ-transition pattern is suitable.

For each resonance a plot was made of each of the $g\Gamma_n$ vs Γ curves implied by the analysis for each sample thickness in transmission and self-indication. The intersection region defined the best choice $(g\Gamma_n, \Gamma)$ value. The methods of the analysis are given elsewhere.[1] An example of the analysis for one level of each isotope is given in Figs. 2(a)–2(d). The resulting level parameters, given in Tables III to VI constitute the body of experimental results of this paper.

The capture width Γ_γ has been determined for a majority of the levels in the Eu isotopes and for some of the levels in the Sm isotopes. An inspection of Figs. 2(c) and 2(d) for the Eu^{151} and Eu^{153} analysis shows that the "D-only" and "flat detector" transmission analyses give nearly the same slopes on a $g\Gamma_n$ vs Γ plot. The curves from the "$D+T$" analysis are nearly orthogonal to the others. This was essential to establish a unique common crossing point in $(g\Gamma_n, \Gamma)$ space.

IV. DISCUSSION OF RESULTS

Probably very few if any p levels are contained in Tables III to VI. The fluctuations of the $g\Gamma_n$ and Γ_γ values, along with the level spacings about their mean values are compared with statistical theories which have been discussed in our previous papers.[1]

A. Samarium

The plots of the cumulative number of observed levels vs energy (N vs E) for Sm^{152} and Sm^{154} are given in Fig. 3. For a complete single s level population, the cumulative number of levels should allow a very good fit by a single straight line. The upper energies where such fits are good are at 3665 eV for Sm^{152} and 3046 eV for Sm^{154}, above which we probably begin to miss a significant number of weak s levels.

Dyson and Mehta[7] introduced a Δ_3 statistic, which we denote simply as Δ, which is the mean squared deviation of $N(E)$ from a best-fit straight line. For a statistical "orthogonal ensemble" (O.E.), they predict that $\langle\Delta\rangle$ should increase only as $\ln(n)$, with a standard deviation of ± 0.11. In addition, the O.E. theory yields an average correlation coefficient of adjacent nearest-neighbor level spacings of $\rho(S_i, S_{i+1})\approx -0.27$. In our previous paper,[8] we showed that a comparison of the experimental values of $[\Delta+\rho(S_i, S_{i+1})]\equiv[\Delta+\rho]$ with that expected

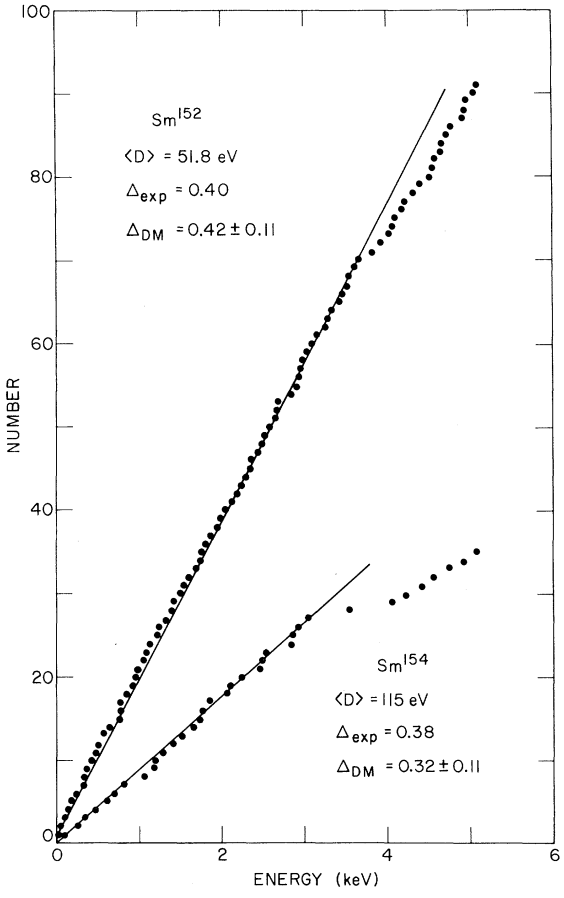

FIG. 3. The cumulative number of observed levels versus E in the Sm isotopes. Good fits to a straight line are obtained up to 3665 eV for Sm^{152} and 3046 eV for Sm^{154}, and the agreement between our Δ_{exp} and the theoretical Δ_{DM} in these energy intervals is shown. Values of $\langle D\rangle$ are obtained from the straight lines.

TABLE III. Resonance parameters for the levels in Sm^{152}. All levels are thought to be $l=0$, with few, if any levels missed below 3700 eV. Asterisk indicates value used in the analysis taken from Ref. 3.

E_0 (eV)	ΔE_0	Γ_n^0 (meV)	$\Delta\Gamma_n^0$	Γ_γ (meV)	$\Delta\Gamma_\gamma$	E_0 (eV)	ΔE_0	Γ_n^0 (meV)	$\Delta\Gamma_n^0$	E_0 (eV)	ΔE_0	Γ_n^0 (meV)	$\Delta\Gamma_n^0$
8.06	0.01	46. *	2.	60	11	1600.6	0.9	8.0	1.2	3288.2	1.3	19.0	2.1
62.2	0.1	0.5	0.3			1691.8	0.5	27.	2.	3315.5	1.4	2.1	0.5
87.7	0.1	22.	2.	65	25	1730.0	0.6	3.4	1.2	3433.5	1.4	19.5	2.0
154.1	0.2	11.4	1.5	93	23	1750.3	0.6	0.2	0.2	3464.0	1.4	7.6	1.2
185.2	0.2	1.4	0.1	51	10	1806.9	0.6	2.4	0.9	3512.0	1.5	11.5	1.5
237.0	0.2	27.	2.			1875.6	0.6	0.2	0.1	3537.8	1.5	41.	5.
314.7	0.3	7.6	1.1			1954.8	0.7	8.8	1.1	3609.4	1.6	2.2	0.7
327.2	0.3	11.3	1.1			1987.0	1.0	0.3	0.2	3665.0	1.6	38.	4.
385.1	0.4	2.0	0.3	45	9	2046.6	0.7	0.6	0.2	3826.6	1.6	4.8	0.6
415.8	0.4	2.8	0.2	58	10	2121.5	0.7	18.5	2.0	3925.7	1.7	11.0	1.4
482.9	0.5	0.4	0.2			2196.7	0.8	0.2	0.1	4028.4	1.7	6.0	0.8
505.9	0.5	8.7	0.7			2237.1	0.8	5.9	0.8	4075.5	1.8	3.4	0.8
587.1	0.5	6.6	0.7	81	24	2310.5	0.9	5.6	0.8	4101.5	1.8	11.9	1.6
641.9	0.5	15.0	0.8			2367.8	0.9	4.1	0.6	4172.6	1.9	63.	6.
768.7	0.6	17.7	0.9			2392.5	0.9	3.7	0.6	4215.3	1.9	8.8	1.2
775.4	0.6	83.	5.			2456.3	1.0	8.1	0.8	4320.3	1.9	15.4	2.0
792.5	0.6	4.1	0.3	60	14	2490.0	1.0	0.2	0.1	4405.0	2.0	0.9	0.4
852.9	0.4	13.5	1.0			2522.0	1.0	0.9	0.4	4523.0	2.0	6.1	0.9
928.7	0.4	0.2	0.1			2582.6	1.0	3.0	0.6	4557.0	2.0	5.6	0.9
952.3	0.4	13.3	1.0			2648.5	1.1	44.	4.	4590.0	2.0	4.1	0.7
986.4	0.5	6.5	0.7			2656.9	1.1	23.	3.	4651.0	2.0	8.2	0.9
1047.6	0.6	6.8	0.8			2695.8	1.1	7.9	1.2	4668.0	2.0	23.	2.
1081.8	0.7	1.0	0.2			2854.0	2.0	0.6	0.2	4725.0	2.0	1.0	0.4
1113.2	0.8	1.1	0.1			2912.1	1.1	25.	3.	4777.0	2.0	7.4	1.0
1228.1	0.6	11.8	0.8			2925.0	1.2	1.1	0.4	4923.0	2.0	10.8	1.6
1239.5	0.6	14.5	0.9			2966.6	1.2	8.4	1.3	4946.0	3.0	5.5	0.9
1314.4	0.6	6.8	0.6	73	25	2985.5	1.2	22.	3.	4985.0	3.0	23.	3.
1402.4	0.7	30.	2.			3030.7	1.2	11.1	1.5	5073.0	3.0	30.	4.
1427.2	0.7	33.	3.			3104.0	2.0	3.2	0.7	5100.0	3.0	3.8	1.0
1501.9	0.8	2.5	0.3			3157.9	1.3	8.7	1.1				
1541.3	0.8	9.9	2.0			3258.7	1.3	9.6	1.2				

TABLE IV. Resonance parameters for the levels in Sm^{154}. All levels are thought to be $l=0$, with few, if any, levels missed below 3000 eV.

E_0 (eV)	ΔE_0	Γ_n^0 (meV)	$\Delta\Gamma_n^0$	Γ_γ (meV)	$\Delta\Gamma_\gamma$	E_0 (eV)	ΔE_0	Γ_n^0 (meV)	$\Delta\Gamma_n^0$	E_0 (eV)	ΔE_0	Γ_n^0 (meV)	$\Delta\Gamma_n^0$
93.0	0.1	14.4	2.0			1556.0	1.0	50.	3.	2862.7	1.1	1.3	0.2
261.1	0.2	9.7	1.3			1647.0	1.0	74.	2.	2987.8	1.2	26.	3.
341.5	0.3	0.8	0.2	65	15	1734.0	0.5	1.9	0.3	3046.8	1.2	26.	3.
457.3	0.4	7.5	0.9	90	25	1768.8	0.6	13.6	0.6	3540.7	1.4	3.0	1.3
617.8	0.5	7.0	0.7			1847.8	0.6	37.	2.	4060.5	1.7	9.3	1.3
704.7	0.5	29.	2.			2056.5	0.7	3.3	0.7	4213.0	1.8	52.	8.
828.7	0.4	108.	7.			2106.9	0.7	53.	3.	4415.0	2.0	57.	8.
1075.5	0.5	0.4	0.1			2243.0	1.5	1.5	0.8	4550.0	2.0	6.2	1.0
1181.5	0.6	2.1	0.1	83	23	2452.2	0.8	27.	3.	4757.0	2.0	33.	4.
1187.7	0.7	0.3	0.2			2492.0	0.9	1.1	0.2	4920.0	2.0	26.	3.
1282.9	0.7	14.2	1.0			2529.5	1.0	51.	15.	5075.0	3.0	17.3	2.4
1472.1	0.8	18.5	1.0			2834.1	1.0	3.6	0.6				

TABLE V. Resonance parameters for the levels in Eu^{151}. $g=\frac{5}{12}$ and $\frac{7}{12}$ for $J=2$ and $J=3$, respectively. Resonance parameters for levels below 1 eV are taken from Ref. 3.

E_0 (eV)	ΔE_0	$g\Gamma_n^0$ (meV)	$\Delta g\Gamma_n^0$	Γ_γ (meV)	$\Delta\Gamma_\gamma$
0.321	0.002	0.08	0.002	80	2
0.461	0.002	0.57	0.01	89	3
1.05	0.005	0.11	0.03		
1.83	0.01	0.01	0.003		
2.71	0.01	0.08	0.01	97	5
3.36	0.01	0.25	0.05	97	6
3.71	0.01	0.21	0.03	89	6
4.78	0.01	0.04	0.005		
5.38	0.01	0.04	0.004	108	12
5.98	0.01	0.07	0.01	100	15
7.05	0.02	0.01	0.01		
7.29	0.02	0.41	0.06	88	12
7.44	0.02	0.31	0.05	85	9
9.07	0.02	0.18	0.02	104	12
10.47	0.03	0.32	0.03	91	9
10.94	0.03	0.10	0.01	98	11
11.23	0.04				
12.23	0.04	0.13	0.01	88	9
12.64	0.04	0.34	0.03	88	7
13.66	0.05	0.06	0.01	115	12
14.76	0.05	0.25	0.01	76	9
15.18	0.05	0.26	0.03	79	9
17.75	0.06	0.16	0.01	104	11
19.10	0.07	0.59	0.05	133	19
19.70	0.07				
21.00	0.07				
21.30	0.07				
21.69	0.07	0.21	0.02	82	12
22.21	0.08	0.30	0.04	66	15
22.75	0.08	0.16	0.01	89	9
24.25	0.09				
24.58	0.09	0.85	0.06	99	10
25.17	0.11	0.06	0.02		
25.60	0.11	0.05	0.02	89	17
26.22	0.12				
26.72	0.12	0.68	0.06	78	10
27.43	0.12	0.06	0.01	97	8
27.75	0.12				
28.09	0.12	0.03	0.01	90	15
29.23	0.05	0.42	0.03	79	11
30.22	0.06	0.33	0.03	86	6
30.81	0.06	0.06	0.01	99	14
31.59	0.06	0.15	0.01	97	7
32.65	0.06				
33.51	0.06	0.04	0.01		
33.88	0.06				
34.57	0.06	0.03	0.01		
35.05	0.07	0.27	0.03	90	8
36.09	0.07	0.42	0.03	78	8
37.01	0.07	0.46	0.03	78	9
37.78	0.07	0.28	0.02	92	7
39.20	0.07	0.08	0.03		
39.37	0.07	0.32	0.05	79	9
39.94	0.08	0.10	0.01	79	9
40.42	0.08				
41.35	0.08	2.10	0.23	80	13
42.12	0.09	0.08	0.03		
43.19	0.09	0.43	0.03	84	9
44.43	0.09	0.27	0.03	89	8
45.42	0.10	0.10	0.02	99	18
46.41	0.10	0.76	0.22	85	19
47.24	0.11	1.24	0.15	99	12
48.75	0.13				
49.23	0.14				
50.04	0.15	0.07	0.03		
50.58	0.12	1.62	0.14	102	11
51.61	0.12				
52.41	0.12	0.28	0.07		
52.70	0.12	0.33	0.07	80	15
53.25	0.13	0.06	0.01		
53.94	0.14	0.31	0.02	88	10
54.90	0.14				
55.26	0.07	0.26	0.02	96	9
56.18	0.07	0.23	0.02	98	9
57.36	0.07	1.25	0.11	83	9
58.85	0.08	0.42	0.04	108	11
60.85	0.08	0.37	0.04	96	9
62.41	0.08	0.25	0.03	86	8
63.19	0.09	0.16	0.03	100	11
67.91	0.10	1.09	0.05	100	10
69.09	0.10	0.06	0.02		
70.75	0.10	0.27	0.04	78	10
71.41	0.10	0.36	0.04	84	10
72.41	0.11	0.13	0.02	93	11
73.33	0.11	0.07	0.02		
74.16	0.11	0.09	0.02		
75.76	0.11	0.24	0.03	90	11
77.45	0.12	0.50	0.03	99	10
78.05	0.12	0.03	0.02		
78.66	0.12	0.96	0.09	73	9
79.51	0.12	0.31	0.04	64	13
80.29	0.12	0.46	0.06	81	10
81.08	0.13	1.33	0.11	101	13
83.07	0.13	0.18	0.02	95	11
84.00	0.13	0.81	0.04	99	12
85.67	0.14	0.26	0.03	84	18
87.70	0.14	0.07	0.02		
88.63	0.14	0.06	0.02		
89.34	0.15	0.77	0.04	104	13
90.18	0.15	0.26	0.03	85	14
91.13	0.15	0.25	0.03	94	11
93.36	0.15	1.45	0.10	112	13
96.29	0.16	0.94	0.10	112	13
97.70	0.16	0.10	0.02		
98.61	0.16	0.78	0.05	108	13

TABLE VI. Resonance parameters for the levels in Eu^{153}. $g=\frac{5}{12}$ and $\frac{7}{12}$ for $J=2$ and $J=3$, respectively. Resonance parameters for levels below 1 eV are taken from Ref. 3.

E_0 (eV)	ΔE_0	$g\Gamma_n^0$ (meV)	$\Delta g\Gamma_n^0$	Γ_γ (meV)	$\Delta\Gamma_\gamma$	E_0 (eV)	ΔE_0	$g\Gamma_n^0$ (meV)	$\Delta g\Gamma_n^0$	Γ_γ (meV)	$\Delta\Gamma_\gamma$	E_0 (eV)	ΔE_0	$g\Gamma_n^0$ (meV)	$\Delta g\Gamma_n^0$	Γ_γ (meV)	$\Delta\Gamma_\gamma$
0.457	0.005	0.007	0.002			34.53	0.06	0.44	0.05	90	12	64.09	0.09	0.87	0.06	116	15
1.73	0.01	0.02	0.002	91	9	36.62	0.07	0.35	0.05	106	14	65.25	0.09				
2.46	0.01	0.35	0.02			37.76	0.07	0.36	0.05	94	12	65.90	0.09				
3.29	0.01	0.20	0.02			38.30	0.07	0.48	0.03	81	11	66.94	0.09	0.23	0.04	86	17
3.94	0.01	0.27	0.02	94	5	41.15	0.08	0.11	0.01	69	20	68.15	0.10	0.31	0.04	87	12
4.75	0.01	0.02	0.005			42.15	0.09	0.37	0.05	77	14	70.04	0.10	0.18	0.02	100	14
6.16	0.02	0.13	0.01	109	10	43.16	0.09	0.24	0.03	96	9	71.35	0.10	0.07	0.01		
8.85	0.02	0.57	0.05	114	11	44.82	0.09	0.05	0.01			73.68	0.11	0.02	0.01		
11.61	0.03	0.65	0.06	96	10	45.79	0.10	0.10	0.01	99	15	75.47	0.11	0.03	0.02		
12.45	0.04	0.02	0.001	90	25	47.11	0.10	0.15	0.01	94	11	76.93	0.11	0.82	0.03	105	13
13.22	0.04	0.05	0.01			47.93	0.11	0.45	0.03			80.29	0.12	0.27	0.03	103	19
15.26	0.05	0.05	0.01			49.30	0.11	0.01	0.01			81.24	0.13	0.22	0.03	96	14
16.33	0.05	0.004	0.002			49.50	0.11	0.02	0.01			82.99	0.13	0.20	0.03	86	9
16.73	0.05	0.17	0.04	89	15	50.00	0.12	0.21	0.02	92	8	84.00	0.13	0.04	0.03		
17.60	0.06	0.07	0.05			50.74	0.12	0.52	0.04	113	14	86.99	0.14	0.66	0.03	68	8
18.01	0.06	0.59	0.05	92	15	52.31	0.13	0.84	0.06	108	15	87.70	0.14	0.26	0.02	105	16
18.73	0.07	0.35	0.05	100	11	53.07	0.14	0.19	0.03	119	14	89.34	0.15	0.07	0.02		
20.02	0.07	1.05	0.07	101	16	54.29	0.14	0.84	0.05			90.75	0.15	0.22	0.02	79	13
22.54	0.08	0.29	0.04	84	12	55.19	0.07	0.02	0.01	95	20	92.01	0.15				
23.66	0.09	0.27	0.04	86	12	55.57	0.07	0.13	0.01			92.80	0.15	0.12	0.06		
26.19	0.20	0.03	0.01			58.40	0.08					93.26	0.15	2.17	0.21	88	20
28.63	0.12	0.17	0.01	79	15	58.97	0.08	0.08	0.01	85	9	94.76	0.15	0.04	0.02		
29.90	0.05	0.03	0.01			59.72	0.08	0.18	0.02	102	15	95.15	0.15	0.12	0.01		
31.21	0.06	0.21	0.02	118	13	60.92	0.08	2.05	0.13	78	14	96.86	0.16	0.15	0.05		
32.45	0.06	0.02	0.01			62.55	0.08	0.33	0.04	105	13	97.60	0.16	1.32	0.30	101	15
33.05	0.06					63.70	0.09	0.46	0.05	93	20						

for the O.E. theory and with that expected from a set of "uncorrelated Wigner" spacings (U.W.) provides a cleaner test of the theory than a comparison with Δ or ρ alone.

For the 70 levels of Sm^{152} to 3665 eV, we obtain $\Delta_{exp} = 0.40$ vs $\Delta_{DM} = 0.42 \pm 0.11$ and $\rho(S_i, S_{i+1}) = -0.26 \pm 0.10$. The experimental value of $[\Delta + \rho]$ is consistent with the O.E. theory but the probability is only 0.004 for less than or equal this experimental value for a U.W. set of spacings. For the 27 levels of Sm^{152} to 3046 eV we obtain $\rho(S_i, S_{i+1}) = -0.34 \pm 0.18$ and $\Delta_{exp} = 0.38$ compared with $\Delta_{DM} = 0.32 \pm 0.11$. The observed $[\Delta + \rho]$ is again consistent with O.E. theory but the probability is 0.10 for less than or equal this value for a U.W. set of spacings.

While the agreement of these experimental results with the O.E. theory is excellent, the discrimination against such alternatives as the U.W. set is less impressive than for Er^{166}, mainly because of the smaller sample sizes. Nevertheless, these results provide valuable supporting evidence in establishing the experimental validity of the O.E. theory for "single level populations" in nuclear spectroscopy at high excitation energy above the low-lying nuclear states.

Since the Sm^{152} and Sm^{154} levels in the indicated energy regions satisfy the above tests, they are probably relatively complete uncontaminated s populations and should also satisfy the Wigner formula for the nearest-neighbor level-spacing distribution and the Porter-Thomas (PT) single-channel theory for the Γ_n^0 distributions. Figures 4(a) and 4(b) show the integrals of the observed nearest-neighbor spacing distribution with the integral of the Wigner formula for comparison. According to Monahan and Rosenzweig[9] the mean square deviation of the theoretical and experimental curves should be less than that for an equal population sample size of adjacent U.W. spacings.

Figure 4(c) shows the values of $\sigma(k)$ versus k for the Sm isotopes. The statistic $\sigma(k)$ is the standard deviation about $(k+1)\langle D\rangle$ of the values for the energy spacing of the levels separated by k other levels. The values for the O.E. and the U.W. cases are shown, as are the 10 and 90% O.E. confidence limits for the number of levels involved in the Sm isotopes. Also shown are the two-body-random-ensemble (TBRE) calculations of Bohigas and Flores.[10] The agreement with the O.E. case is excellent and quite different from the mean values shown for the U.W. or TBRE cases.

The observed distributions for the $(\Gamma^0{}_n)^{1/2}$ values are given in Figs. 5(a) and 5(b). The results are in reasonable agreement with the (PT) single-channel theory.

The average level spacing is expected to have a fractional statistical uncertainty $\approx 1/n$ for an O.E. To include possible single-population-sample imperfections of our level sets, we give $2/n$ fraction-

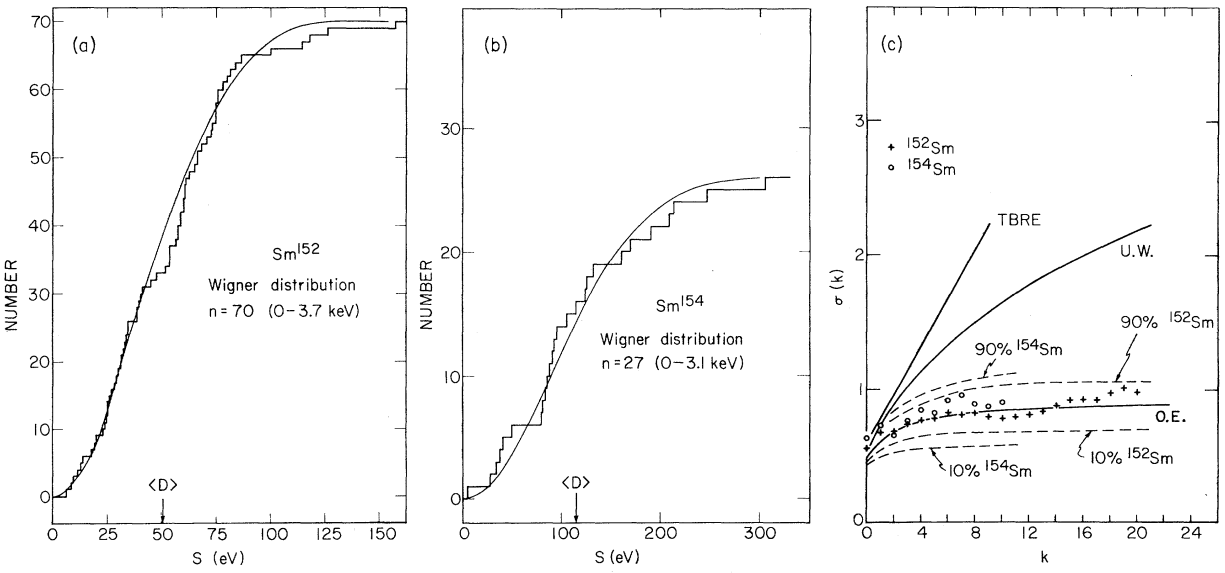

FIG. 4. (a), (b) Cumulative histogram of the observed nearest-neighbor spacing distribution in the energy intervals over which few, if any, levels have been missed for Sm^{152} and Sm^{154}, respectively, with the integral of the Wigner distribution shown as a comparison. (c) $\sigma(k)$ versus k for the Sm isotopes. The theoretical curves are for the two-body random ensemble (TBRE), the uncorrelated Wigner (U.W.), and the orthogonal ensemble (O.E.). Our experimental data are consistent with the O.E., shown with 10–90% confidence limits, and quite different from the TBRE and U.W. curves.

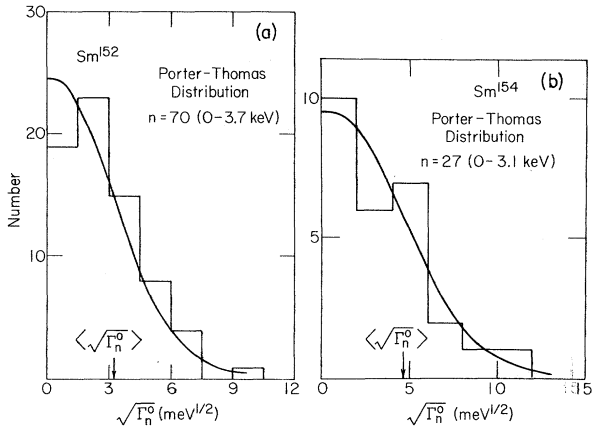

FIG. 5. (a), (b) The histogram of the observed distributions of $\sqrt{\Gamma_n^0}$ for the Sm isotopes. The curves are normalized to the observed strength function S_0. There is excellent agreement between the histograms and the theoretical Porter-Thomas curve for the reduced neutron widths.

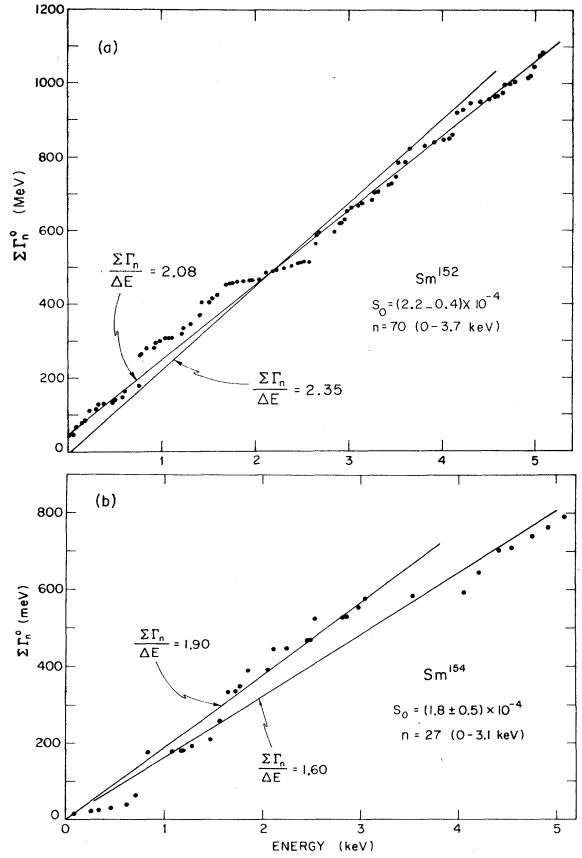

FIG. 6. (a), (b) Plots of $\Sigma\Gamma_n^0$ versus E for the Sm isotopes. The slope of the curves give the $l = 0$ strength function. Each figure shows two curves which are extreme choices for S_0. Out best choice lies between these curves and is indicated on the figure.

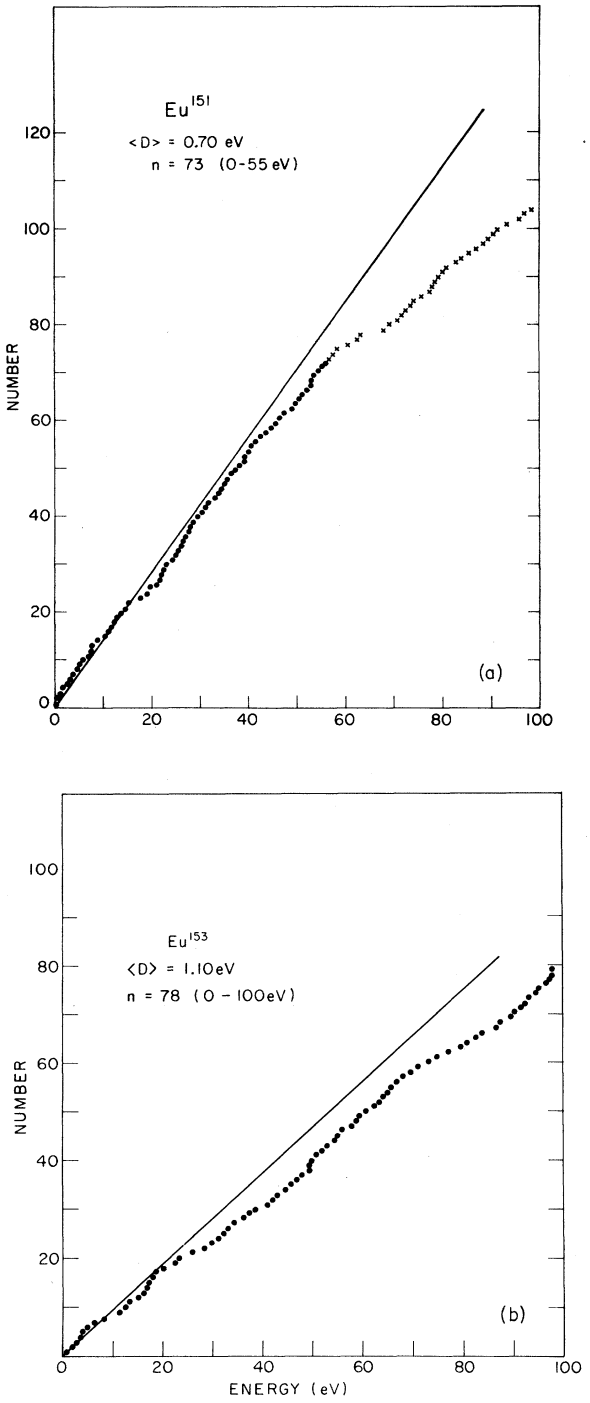

FIG. 7. (a), (b) Cumulative number of observed levels in the Eu isotopes. The decreasing density of observed levels as the energy increases is on account of levels missed because of the small mean spacing between levels and the absence of the Wigner repulsion effect for the two spin populations in each isotope. The straight line indicated on these figures are our estimate of $\langle D \rangle$, the mean level spacing.

al uncertainties so $\langle D\rangle = 51.8 \pm 1.5$ eV for Sm^{152} and 115 ± 8 eV for Sm^{154}.

The s-level strength functions, S_0, are obtained from the slopes of the plots of $\sum\Gamma_n^0$ vs E shown in Figs. 6(a) and 6(b) for Sm^{152} to 5.1 keV (90 levels) and Sm^{154} to 5.1 keV (33 levels). The figures each show two straight lines which nearly represent extremes as to how one might fit the slope, noting that the Γ_n^0 evaluations are expected to be somewhat more reliable at the lower-energy regions. In Sm^{154}, the region between 3 and 4 keV contains only levels with small Γ_n^0, so that the 4- to 5-keV region lies below the trend of the 0- to 3-keV region. The strong contribution from the 8.06-eV level in Sm^{152} leads to a best-fit straight line with a positive intercept at $E = 0$ with a good fit over the region using a value of $10^4 S_0 = 2.04$. Our best choices for the s-wave strength function are:

Sm^{152}: $10^4 S_0 = 2.2 \pm 0.4$, $n = 70$ levels;

Sm^{154}: $10^4 S_0 = 1.8 \pm 0.5$, $n = 27$ levels.

The fractional uncertainties are approximately $(2/n)^{1/2}$ due to statistical considerations alone.

For some favorable cases, we were able to obtain Γ_γ. We found $\langle\Gamma_\gamma\rangle$ to be 65 meV for 9 levels in Sm^{152} and 79 meV for 3 levels in Sm^{154}. These values of $\langle\Gamma_\gamma\rangle$ for the Sm isotopes are somewhat lower than those that we obtain for Eu, but our evaluated capture-resonance integrals using $\langle\Gamma_\gamma\rangle$ for levels where Γ_γ was not obtained are in agreement with experimentally determined values.[11]

B. Europium

Figures 7(a) and 7(b) show the cumulative number of observed levels versus energy for the Eu isotopes. Because of the small p-wave strength function for $A = 150$, the slope of the curves in Fig. 7 should be due only to s levels. The decreasing slope as the energy increases is due to our missing an increasing fraction of the levels at higher energy because of the small mean spacing and the absence of the Wigner repulsion effect for levels of different J. The decreasing slope of $N(E)$ for Eu^{151} below the value of $\langle D\rangle = 0.70$ eV which fits for the first 15 eV would be greater if less-certain levels were included. The true $\langle D\rangle$ is probably about 0.7 eV, but may be as low as 0.6 eV or a little smaller. The slope for Eu^{153} is $\langle D\rangle = 1.1$ to 20 eV with a subsequent decrease which, however, is not monotonic above 20 eV. The higher initial slope to 5 eV, followed by a reduced density of observed levels between 5 and 11 eV is puzzling but is indicated by the data. A true value of $\langle D\rangle$ of 1.0 to 1.1 eV seems most probable.

Figure 8 shows the histograms of the nearest-neighbor distribution for the Eu isotopes for the energy intervals 0–55 eV for Eu^{151} and 0–100 eV for Eu^{153} over which relatively complete level populations exist. Also shown on this figure is the theoretical Wigner distribution for two spin populations. For the Wigner distribution we have assumed that the level densities of the two spin populations are approximately equal from the ratio of the statistical spin factors $g_+ \cong g_- \cong \frac{1}{2}$. The Wigner two-population curves are completely determined by the energy-interval size and assumed $\langle D\rangle$. If the observed histogram was to be corrected to take into account missed spacings, the qualitative effect would be to divide, usually asymmetrically each erroneous single spacing into two smaller spacings. This would tend to increase the relative number of small spacings. Wigner curves are given for $\langle D\rangle = 0.6$ and 0.7 eV for Eu^{151} and 1.1 eV for Eu^{153}. These values are reasonable, considering the effects of missing levels, and a value of $\langle D\rangle = 0.7$ eV is slightly favored for Eu^{151}.

For an odd-A nucleus, where the J value of each individual level is not established (the Eu case), we obtain a weighted average contribution from the two spin states to the strength function. If subscripts 1 and 2 denote the different J cases, the S_0 value for the separate J states would be $\langle\Gamma_n^0\rangle_1/\langle D\rangle_1$ and $\langle\Gamma_n^0\rangle_2/\langle D\rangle_2$. The level densities for the two spin states tend to be in proportion to the $(2J+1)$ values of the g_J values of the two spins, where $g_1\langle D\rangle_1 \cong g_2\langle D\rangle_2 \cong \langle D\rangle$. For the analysis we used the weighted average of $\langle g\Gamma_n^0\rangle_1$ and $\langle g\Gamma_n^0\rangle_2$ by using $\sum g\Gamma_n^0/\Delta E$, where ΔE is the energy interval considered. If $S_{01} \cong S_{02} \cong S_0$, then $\langle g\Gamma_n^0\rangle_1 \cong \langle g\Gamma_n^0\rangle_2 \cong \langle g\Gamma_n^0\rangle$ and the $g\Gamma_n^0$ values have a common PT distribution. Recent data from Saclay[12] indicate that the s strength function is spin-dependent for certain of the rare-earth isotopes. However, the Saclay data on the Gd^{155} and Gd^{157} isotopes (both with spin $I = \frac{3}{2}$) did not exhibit any strong spin dependence of S_0. One would expect, therefore, at most a small spin dependence for the Eu isotopes, with a much greater effect possibly in the mass region of the Nd isotopes, $A \simeq 144$. From the slopes of $\sum g\Gamma_n^0$ in Figs. 9(a) and 9(b), S_0 is $(3.2 \pm 0.5) \times 10^{-4}$ for Eu^{151} (from 0 to 55 eV) and $(2.3 \pm 0.4) \times 10^{-4}$ for Eu^{153} (from 0 to 100 eV). For Eu^{151}, S_0 taken over the interval 0–100 eV is 3.25×10^{-4} which is quite close to the value for the interval 0–55 eV where our data are least influenced by experimental resolution. Our values of $g\Gamma_n^0$ in Table V for Eu^{151} above 55 eV are considered to be somewhat less reliable in that some of the resonances that we have listed may be actually two or more unresolved levels, and there appears to be a substantial number of missing levels in this energy region according to Fig. 7(a). Seth[13] has recommended the values $10^4 S_0 = 2.4 \pm 0.7$ for

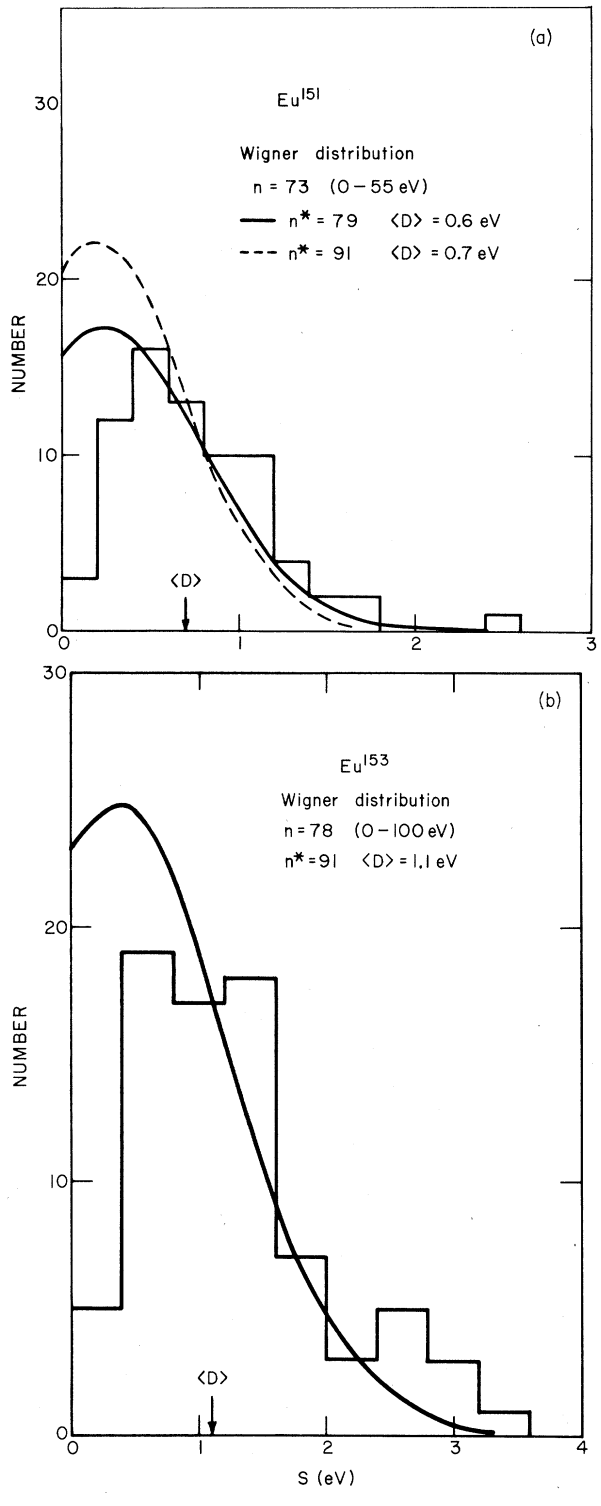

FIG. 8. (a), (b) Histograms of the observed nearest level spacings, S, for the Eu isotopes. The curves are the theoretical Wigner distributions for two randomly positioned populations with equal level densities. Two possible choices of $\langle D \rangle$ are shown for Eu^{151}.

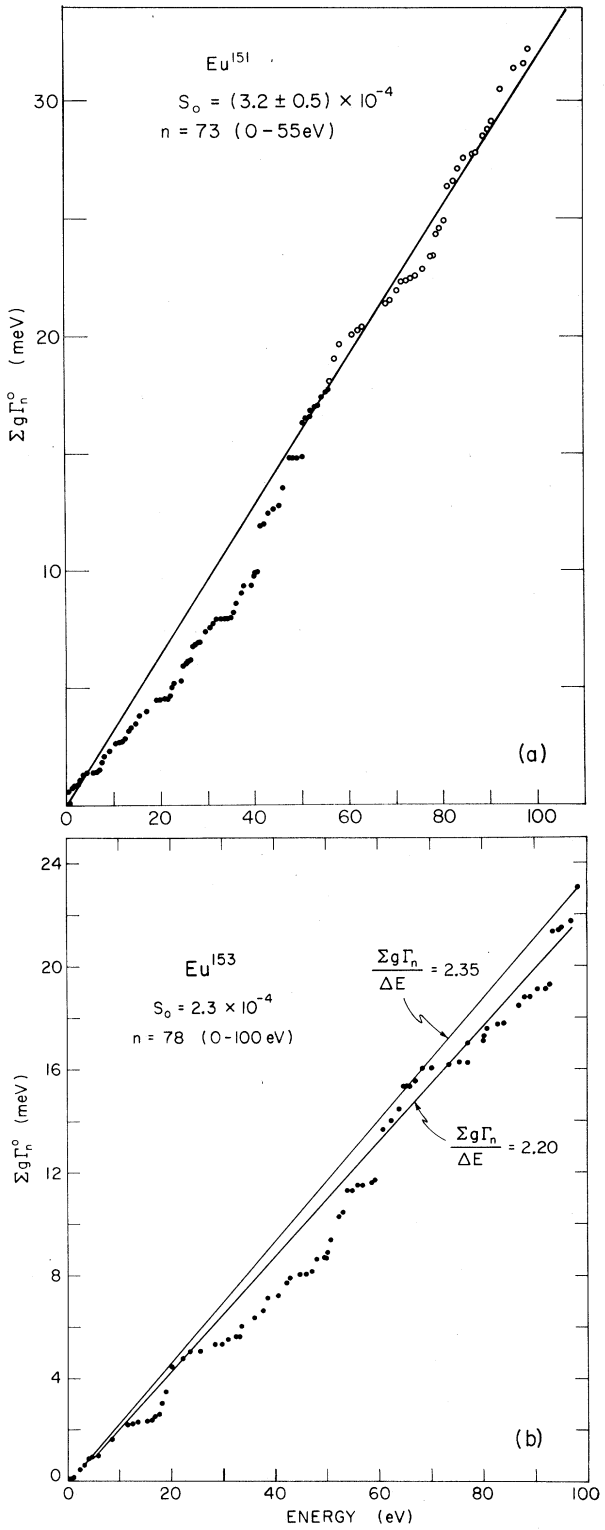

FIG. 9. (a), (b) Plots of $\Sigma g \Gamma_n^0$ for the Eu isotopes. We determine the $l = 0$ strength function from the slope of the curves, and have assumed that the strength functions for the different spin states ($J = 2$ and 3) are essentially equal.

Eu^{151} and 2.2 ± 0.7 for Eu^{153}. The agreement is close for Eu^{153} but poorer for Eu^{151}. This is due to his use of average cross-section measurements combined with individual resonance results for a smaller level sample. Note that Fig. 9(a) would give about 2.4 for the interval below 40 eV for Eu^{151}.

Figure 10 shows the distribution of the observed reduced neutron widths for the Eu isotopes. The histograms are plotted as the number of observed levels versus $\sqrt{g\Gamma_n^0}$ for all levels below 55 eV for Eu^{151} and 100 eV for Eu^{153} with a histogram interval of 0.2 $meV^{1/2}$. Also shown is the theoretically favored PT distribution, normalized in each case to our observed value of the strength function. We have drawn two curves for each of our PT distributions, one curve for the number of levels, n, actually observed in the indicated interval; the other curve for the maximum number of levels, $n^* = \Delta E/\langle D\rangle$, that we would expect from our lowest possible value of $\langle D\rangle$. In the usual situation where $\langle D\rangle \gg 1$ eV, the missing of s levels tends to be based on their being too weak. For $\langle D\rangle \leq 1$ eV, as for Eu, "missing levels" are more apt to be an effect of treating two overlapping levels, usually of different J, as one level with approximately the sum of the strengths. The correction for this experimental deficiency would involve breaking some of the $g\Gamma_n^0$ values into two smaller values. With this effect considered, the observed differences between the histograms and the PT curves are plausible.

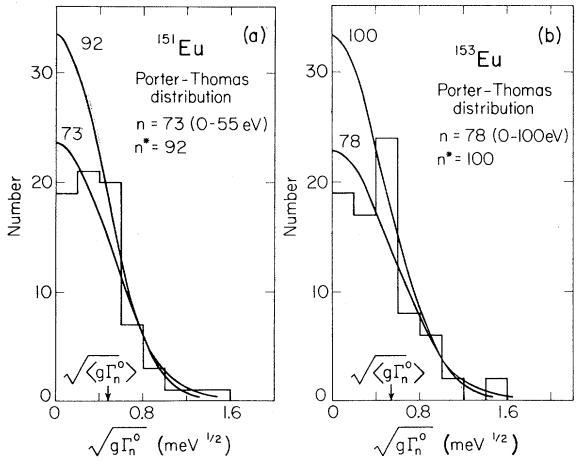

FIG. 10. (a), (b) The distribution of the observed reduced neutron widths for the Eu isotopes, plotted as a function of $\sqrt{g\Gamma_n^0}$ in 0.2-$meV^{1/2}$ intervals. Also shown is the Porter-Thomas distribution for two different possible level densities: n, the observed number of levels; and n^*, the assumed number of levels in the given energy interval.

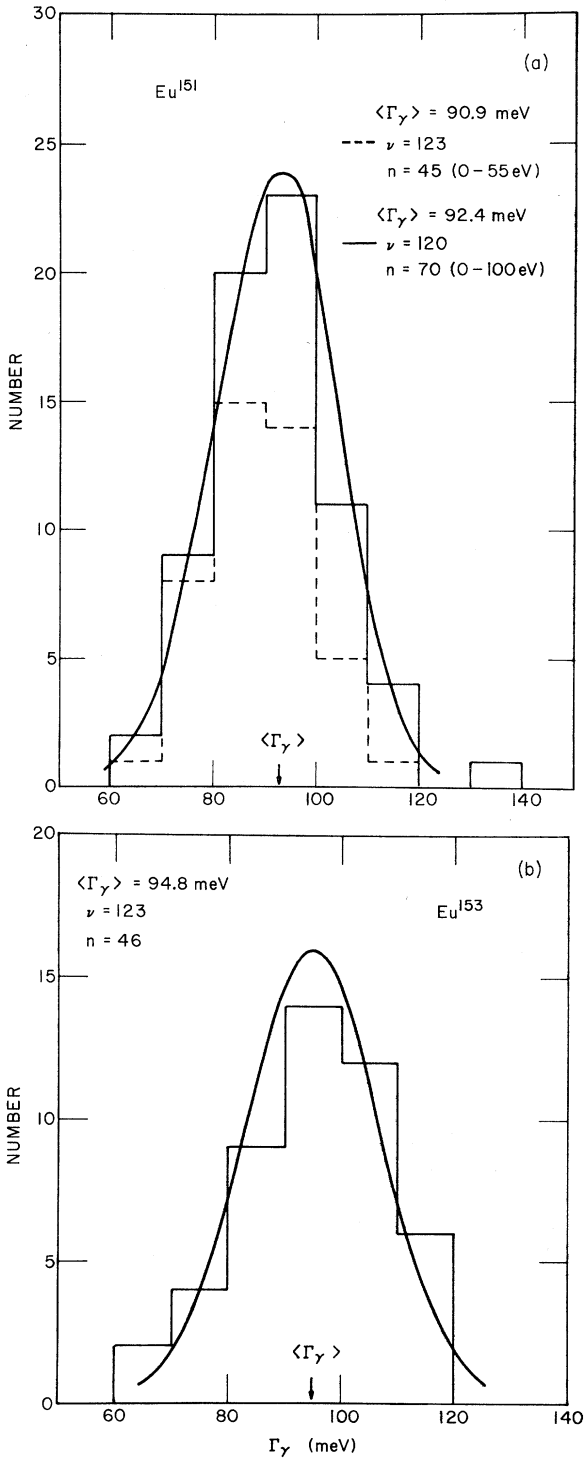

FIG. 11. (a), (b) The distribution of our Γ_γ values for the Eu isotopes. The χ^2 distribution of ν degrees of freedom is also plotted where ν is determined from the analysis, which indicates that a large number of channels are involved in each case.

The total radiation width $\Gamma_{\gamma i}$ for a heavy nucleus is made up of the sum of all of the partial transition widths from the initial state i to all lower states j, $\Gamma_{\gamma i} = \sum \Gamma_{\gamma ij}$. Each of the separate $\Gamma_{\gamma ij}$ is expected to have a PT single-channel distribution about its average, for fixed j, but varying i. When considering the distribution for $\Gamma_{\gamma i}$ about $\langle \Gamma_\gamma \rangle$, the usual analysis neglects the variation (over i) of the $\langle \Gamma_{\gamma j} \rangle$ to particular final states j. A χ^2 fit to the measured $\Gamma_{\gamma i}$ distribution is made,

$$2/\nu = (\langle \Gamma_\gamma{}^2 \rangle - \langle \Gamma_\gamma \rangle^2)/\langle \Gamma_\gamma \rangle^2 ,$$

where the measured averages are used and ν is the effective number of degrees of freedom. Note that ν is inversely proportional to the square of the fractional spread. Part of the observed spread comes from measurement uncertainties which tend to reduce ν below that which would result if there were no measurement errors. Another reduction in ν comes from the fact that transitions to final states having larger than average $\langle \Gamma_{\gamma j} \rangle$ outweigh those of weaker $\langle \Gamma_{\gamma j} \rangle$, so the ν obtained from the analysis tends to be less than the actual number of channels j present even if there were no measurement errors. The measured values of ν are thus a lower limit to the number of capture channels, which may be 1 or 2 orders of magnitude larger than our measured values.

We were able to determine Γ_γ for 45 levels in Eu^{151} to 55 eV (70 levels to 100 eV, although some of the levels between 55 and 100 eV may be doublets, yielding less reliable Γ_γ values), and for 46 levels in Eu^{153}. Figure 11 shows the distributions of the Γ_γ values for the Eu isotopes along with "best fit" χ^2 curves. As expected, the analysis indicates that large effective numbers of channels are involved in each case: $\nu = 123$ for Eu^{151} to 55 eV ($\nu = 120$ for all levels to 100 eV), and $\nu = 123$ for Eu^{153}. We obtain $\langle \Gamma_\gamma \rangle = 90.0$ meV for Eu^{151} to 55 eV, $n = 45$ (90.4 meV to 100 eV, $n = 70$) and 94.8 meV for Eu^{153}, $n = 46$. The fact that two levels are sometimes counted as one probably has no serious effect on our Γ_γ determinations for the following reasons: (1) The missing levels most likely occur where a weak level of one spin state overlaps a stronger one of different J; (2) the analysis curves indicate that $g\Gamma_n$ is well established for each level, which is linear in the level strength, so the $g\Gamma_n$ for two levels treated as one would be essentially the sum of the two values; (3) an area rather than a shape analysis tends to emphasize the stronger contributor and gives an essentially correct value for its Γ_γ. The high effective ν value obtained support this conclusion, since wider observed distributions would have been obtained if considerably different Γ_γ were obtained for unresolved level cases.

ACKNOWLEDGMENTS

We wish to thank Dr. George Rogosa and the U. S. Atomic Energy Commission for help in procuring the separated isotope samples. Dr. Hugo Ceulemans made a substantial contribution in the preparation and data-accumulation phases of the experiment. To the other nonscientific members of the group, Arthur Blake, Lester Morganstein, William Van Wort, and Warren Marshall, we owe a special word of thanks. John Ostrowski was responsible for the preparation of our separated isotopic samples. We also thank Easter Kelly for typing the manuscript, and Frank Da Cruz for preparing the tables.

---

*Research supported by the U. S. Atomic Energy Commission.

†Present address: National Bureau of Standards, Gaithersburg, Md.

‡Present address: Brooklyn College, New York, N. Y.

[1]Earlier papers in this series: I, J. L. Rosen, J. S. Desjardins, J. Rainwater, and W. W. Havens, Jr., Phys. Rev. 118, 687 (1960), U^{238}; II, J. S. Desjardins, J. L. Rosen, W. W. Havens, Jr., and J. Rainwater, *ibid.* 120, 2214 (1960), Ag, Au, Ta; III, J. B. Garg, J. Rainwater, J. S. Petersen, and W. W. Havens, Jr., *ibid.* 134, B985 (1964), Th^{232}, U^{238}; IV, J. B. Garg, W. W. Havens, Jr., and J. Rainwater, *ibid.* 136, B177 (1964), As, Br; V, J. B. Garg, J. Rainwater, and W. W. Havens, Jr., *ibid.* 137, B547 (1965), Nb, Ag, I, Cs; VI, S. Wynchank, J. B. Garg, W. W. Havens, Jr., and J. Rainwater, *ibid.* 166, 1234 (1968), Mo, Sb, Te, Pr; VII, J. B. Garg, J. Rainwater, and W. W. Havens, Jr., Phys. Rev. C 3, 2447 (1971), Ti, Fe, Ni; VIII, H. I. Liou, H. Camarda, S. Wynchank, M. Slagowitz, G. Hacken, F. Rahn, and J. Rainwater, *ibid.* 5, 974 (1972), Er.

[2]F. J. Rahn, Ph.D. thesis, Columbia University, 1970 (unpublished).

[3]*Neutron Cross Sections*, compiled by M. Goldberg *et al.*, Brookhaven National Laboratory Report No. BNL-325 (U. S. GPO, Washington, D.C., 1966), 2nd ed., Suppl. 2.

[4]E. Karzhsvina, N. Fong, and A. Popov, Joint Institute for Nuclear Research Report No. P3-3882, 1968 (unpublished).

[5]D. Chase, L. Wilets, and A. Edmonds, Phys. Rev. 110, 1080 (1958).

[6]W. E. Pineo, private communication.

[7]A series of papers by F. J. Dyson alone and with M. L. Mehta are: I, F. J. Dyson, J. Math. Phys. 3, 140, 157, 166, 1199 (1962); II, M. L. Mehta and F. J.

Dyson, *ibid.* 4, 701, 713 (1963).
[8]H. Liou, H. S. Camarda, and F. Rahn, Phys. Rev. C 5, 1002 (1972).
[9]J. E. Monahan and N. Rosenzweig, Phys. Rev. C 1, 1714 (1970).
[10]O. Bohigas and J. Flores, in *Proceedings of the International Conference on Statistical Properties of Nuclei, Albany, New York, August 23–27, 1971* (Plenum, New York, 1972), p. 195.
[11]F. Rahn, H. Camarda, G. Hacken, W. W. Havens, Jr., H. I. Liou, J. Rainwater, M. Slagowitz, and S. Wynchank, to be published.
[12]C. M. Newstead, J. Delaroche, and B. Cauvin, in *Proceedings of the International Conference on Statistical Properties of Nuclei, Albany, New York, August 23–27, 1971* (see Ref. 10), p. 367.
[13]K. Seth, Nucl. Data A2, 299 (1966).

PHYSICAL REVIEW C VOLUME 6, NUMBER 1 JULY 1972

Nuclear Levels in ^{233}Th Excited by Neutron Capture and (d, p) Reactions*

T. von Egidy, O. W. B. Schult, and D. Rabenstein
Physik-Department, Technische Universität München, München, Germany

and

J. R. Erskine
Argonne National Laboratory, Argonne, Illinois 60439

and

O. A. Wasson and R. E. Chrien
Brookhaven National Laboratory, Upton, New York 11973

and

D. Breitig, R. P. Sharma,† H. A. Baader, and H. R. Koch‡
Physik-Department, Technische Universität München, München, Germany, and Research Establishment Risö, Risö, Denmark
(Received 29 February 1972)

Low-energy γ rays of the reaction ^{232}Th$(n,\gamma)^{233}$Th have been measured with the Risö bent-crystal spectrometer and with a Ge(Li) spectrometer at Munich. High-energy neutron-capture γ rays from four low-energy neutron resonances have been investigated at the fast-chopper facility at Brookhaven. Data on the reaction ^{232}Th$(d,p)^{233}$Th were taken with an Enge split-pole magnetic spectrograph at the tandem Van de Graaff accelerator at Argonne. The combination of these data resulted in a level scheme of ^{233}Th. Seven Nilsson configurations have been assigned to rotational bands, two of them tentatively. Spectroscopic factors have been calculated with ϵ_4 deformation and Coriolis mixing, and compared with the experiment. The neutron binding energy in ^{233}Th has been determined to be 4786.5± 2.0 keV.

1. INTRODUCTION

The deformed nucleus ^{233}Th is supposed to have a structure similar to its isotone ^{235}U. The best ways of investigating ^{233}Th are by means of the (d,p) and (n,γ) reactions. Because of the rather small neutron capture cross section of ^{232}Th (7.4 b), previous (n,γ) experiments[1-6] did not result in a level scheme of ^{233}Th. The (d,p) reaction has recently been measured at Risö.[7]

To obtain more information on ^{233}Th, experiments have been carried out at Risö, Denmark, through the study of low-energy neutron-capture γ rays with a crystal spectrometer, at Munich with a Ge(Li) spectrometer for low-energy capture γ rays, at Brookhaven National Laboratory (BNL), where high-energy γ rays from resonant neutron capture have been investigated, and at Argonne with the (d,p) reaction. Preliminary results have been reported already.[8,9]

An attempt was made to measure conversion electrons following neutron capture with the β spectrometer at the Munich FRM reactor[10] and with the superconducting β spectrometer SULEIKA at the Munich FRM reactor.[11] Because of the low capture cross section, only conversion-electron lines with an intensity of more than about 5 per 100 captures should have been observed. No ^{233}Th lines were found in the conversion-electron spectra.